• Clinical Research •

A new diagnostic model of primary open angle glaucoma based on FD-OCT parameters

Ya-Jie Zheng[1], Ying-Zi Pan[2], Xue-Ying Li[2], Yuan Fang[2], Mei Li[2], Rong-Hua Qiao[2], Yu Cai[2]

[1]Department of Ophthalmology, MEM Eye Care System, Beijing 100039, China
[2]Department of Ophthalmology, Peking University First Hospital, Beijing 100034, China
Correspondence to: Ying-Zi Pan. Department of Ophthalmology, Peking University First Hospital, No.8 Xishiku Street, Xicheng District, Beijing 100034, China. panyingZ123@163.com
Received: 2017-07-20 Accepted: 2018-04-04

Abstract

• AIM: To build a clinical diagnostic model of primary open angle glaucoma (POAG) using the normal probability chart of frequency-domain optical coherence tomography (FD-OCT).

• METHODS: This is a cross-sectional study. Total 133 eyes from 133 healthy subjects and 99 eyes from 99 early POAG patients were included in the study. The retinal nerve fibre layer (RNFL) thickness parameters of optic nerve head (ONH) and RNFL3.45 scan were measured in one randomly selected eye of each subject using RTVue-100 FD-OCT. Then, we used these parameters to establish the diagnostic models. Four different diagnostic models based on two different area partition strategies on ONH and RNFL3.45 parameters, including ONH traditional area partition model (ONH-T), ONH new area partition model (ONH-N), RNFL3.45 traditional area partition model (RNFL3.45-T) and RNFL3.45 new area partition model (RNFL3.45-N), were built and tested by cross-validation.

• RESULTS: The new area partition models had higher area under the receiver operating characteristic (AROC; ONH-N: 0.990; RNFL3.45-N: 0.939) than corresponding traditional area partition models (ONH-T: 0.979; RNFL3.45-T: 0.881). There was no statistical difference among AROC of ONH-T, ONH-N, and RNFL3.45-N. Nevertheless, ONH-N was the simplest model.

• CONCLUSION: The new area partition models had higher diagnostic accuracy than corresponding traditional area partition models, which can improve the diagnostic ability of early POAG. In particular, the simplest ONH-N diagnostic model may be convenient for clinical application.

• KEYWORDS: primary open angle glaucoma; optical coherence tomography; ethnic-specific database; diagnostic model

DOI:10.18240/ijo.2018.06.09

Citation: Zheng YJ, Pan YZ, Li XY, Fang Y, Li M, Qiao RH, Cai Y. A new diagnostic model of primary open angle glaucoma based on FD-OCT parameters. *Int J Ophthalmol* 2018;11(6):951-957

INTRODUCTION

Glaucoma is the second largest cause of bilateral blindness in the world, affecting over 67 million people worldwide[1]. Among glaucoma, the most common form is primary open angle glaucoma (POAG) which is characterized by the loss of retinal ganglion cells and their axons, and affects 33 million individuals worldwide[2-4]. Study has implied that loss of retinal nerve fibre layer (RNFL) and lesion in optic disc may exist even prior to the occurrence of visual defect in glaucoma patients[5]. Therefore, early diagnosis and active treatment are very important in prevention and control of POAG.

Optical coherence tomography (OCT) is a high resolution glaucoma imaging device capable of RNFL and visual function measurements, which has been widely applied in recent years in the diagnosis of many ocular disorders due to its advantages of non-contact and non-invasive[6-8]. With the improvements of the fourth generation of OCT, the resolution and reproducibility of OCT increase gradually, comparing with previous generations[9-13]. Specially, frequency-domain (FD)-OCT has even built an ethnic-specific database of the healthy, based on which a normal probability chart is provided, in favor of the clinical diagnosis of POAG[14]. However, the present normal probability chart can only reflect the normal probability of each selected area instead of the probability of having glaucoma for single individual. Additionally, it is well known that retina nerve fiber in different area has different susceptibility to glaucomatous damage. The change of structural parameters in different locations has quite different weights in glaucoma diagnosis, especially in the early stage. Our previous study has collected data from 99 early POAG and 133 healthy volunteers to build a diagnostic model of primary POAG using the FD-OCT ethnic-specific database of normal humans[15]. In that study, the diagnostic model was established (ONH=OSTITI:2+CA) based on multi-parameters [RNFL, optic nerve head (ONH), and ganglion cell complex (GCC)], which was relatively complicated.

In the present study, we aimed to use two glaucoma scanning programs, ONH and RNFL3.45, in FD-OCT (RTVue-100, software version 6.1, Optovue, Fremont, CA, USA) to detect the RNFL thickness of the same patients and healthy volunteers. We proposed two area partition strategies and grading strategy for the parameters based on the normal probability chart provided by the ethnic-specific normative database to build a more effective and simple diagnostic model for early POAG.

SUBJECTS AND METHODS

Subjects and Samples This is a cross-sectional study. From July 2013 to March 2014, the patients diagnosed as early POAG in the follow-up examination at the specialty outpatient department in Peking University First Hospital (PUFH) were included in this study, including POAG patients with high pressure glaucoma (HPG) and normal tension glaucoma (NTG). The normal control group consisted of volunteers recruited from July 2013 to March 2014 in Beijing. This study followed the principles of the Declaration of Helsinki and was approved by Ethics Committee of PUFH.

The inclusion criteria for healthy volunteers were: 1) the best corrected visual acuity ≥0.8; 2) diopter: sphere -6.00S to +4.00S and cylinder -3.00C to +3.00C, and an isometropia ≤2D; 3) with normal chamber depth, transparent dioptric media, and normal fundus; 4) with healthy optic disc appearance, cup-to-disc ratio (C/D) <0.6, no evidence of diffuse or focal rim thinning, cupping, optic disk hemorrhage, or RNFL defects, interocular asymmetry of C/D<0.2; 5) intraocular pressure tested by applanation tonometer ≤21 mm Hg (1 mm Hg= 0.133 kPa), and central corneal thickness (CCT) between 520 μm and 580 μm; 6) with normal visual field, and determined as "within normal limits" by glaucoma hemi field test (GHT); 7) without family history of glaucoma; 8) without history of retina diseases, optic neuropathy, uveitis, eye trauma and intraocular surgery; 9) without diabetes, high blood pressure or any other systematic diseases that had potential influence on the results of measurement; 10) age >18y.

The inclusion criteria for early POAG patients were: 1) the best corrected visual acuity ≥0.8; 2) diopter: sphere -6.00S to +4.00S and cylinder -3.00C to +3.00C, and an isometropia ≤2 D; 3) the anterior chamber angel was open; 4) C/D≥0.6, or C/D difference between two eyes ≥0.2 with enlarged and deepened optic cup, and a notch along the border of the optic disc (or disappearance of disc border or hemorrhage along disc border) with loss of fibrous layer of the retina nerve in the corresponding positions, as determined by experienced glaucoma specialties inspecting the color stereographs; 5) with at least twice repeatable characteristic findings of visual defect of early glaucoma, with visual field mean deviation (MD) ≥-6 dB; suggested as "outside normal limits" by GHT; presence of paracentral scotoma or the normality probability <0.05 in at least three clusters at nasal side and <0.01 in more than one clusters as revealed by pattern deviation probability plots; or patients diagnosed as glaucoma normal in examination on visual field, but with characteristic glaucoma alteration in visual defect at the fellow eye, with C/D ≥0.6 in the eye with normal visual field, or C/D difference between two eyes ≥0.2, with enlarged and deepened optic cup with notch along disc border (or disappearance of disc border or hemorrhage along disc border) with loss in the fibrous layer of retina nerve in the corresponding locations; 6) without history of retina diseases, optic neuropathy, uveitis, or eye trauma; 7) without history of anti-glaucoma surgery or laser therapy within one year; 8) without diabetes, high blood pressure and any other systematic diseases which might influence the outcome of measurement; 9) age >18y.

A total of 133 eyes from 133 healthy subjects and 99 eyes from 99 early POAG patients were included in the study. We randomly selected 90 normal eyes and 60 early POAG eyes to construct modeling samples. The remaining samples, including 43 normal eyes and 39 early POAG eyes, were used as test samples to verify the diagnostic model.

Disease History Inquiry and Routine Ophthalmological Examination Routine ophthalmological examinations included eyesight and optometry examination (mydriatic optometry was performed for subjects <40 years old), slit-lamp examination, fundus examination with direct ophthalmoscope, Goldmann applanation tonometry, and gonioscope examination.

Visual Field Examination Visual field examination was performed using a Humphrey perimeter (Humphrey Field Analyzer model 750i; Carl Zeiss Meditec, Dublin, CA, USA) with the SITA rapid 24-2 program. The results were considered reliable if they were consistent with the following criteria: 1) fixation loses <20%; 2) both false positive rate and false negative rate <30%.

Optical Coherence Tomography Examination Optovue RTVue100 (software version 6.1; Optovue, Fremont, CA, USA) FD-OCT was used for the OCT examination. The scanning wavelength of RTVue-100 was 840±10 nm, with the depth of the scanning area of 2-2.3 mm, length of 2-12 mm, longitudinal resolution of 5 μm, transverse resolution of 15 μm and scanning speed of 26 000 A-scans/s.

The scanning was performed under non-mydriatic condition in internal fixation, and "China" was selected for the race. Three scanning models, including MM6/Radial Slicer, ONH, and RNFL3.45, were used for each subject. Images scanned were stored if they were complete, with signal strength indicator (SSI) ≥35 and clear fundus image, and without strong reflection.

Fundus Color Photography A Topcon TRC-ss fundus color stereo camera was used for vectograph of fundus in patients with early POAG. Mydriasis was induced by the instillation

of 0.5% compound tropicamide by an experienced technician. The photos were read by a glaucoma specialist.

Determination of Colors for the Scanning Parameter When the RNFL thickness of patients determined by OCT were beyond the normal range compared with the database, the result would be marked with a specific color by the software in the report. Those with normal distribution probability less than 5% were marked as yellow (critical status), and those with normal distribution probability less than 1% were market as red (abnormality). A database of Chinese race was used in this research, and a correction had been made on the age and size of optic disc in this database.

Area Partition Strategies Area partition was performed for RNFL thickness parameters of RNFL3.45 and ONH scan. They were divided into 16 sectors and combined into 6 regions (with 4 sectors for each): the superior temporal and the inferior temporal (STIT) included IT1, IT2, ST1 and ST2; the superior nasal and inferior nasal (SNIN) included SN1, SN2, IN1 and IN2; the superior temporal and superior nasal (STSN) included ST1, ST2, SN1 and SN2; the inferior temporal and the inferior nasal (ITIN) included IT1, IT2, IN1 and IN2; the temporal upper and temporal lower (TUTL) included TU1, TU2, TL1 and TL2; the nasal upper and the nasal lower (NUNL) included NU1, NU2, NL1 and NL2. The traditional partition included STSN, ITIN, TUTL and NUNL. The new partition included: STIT, SNIN, TUTL and NUNL (Figure 1).

Statistical Analysis In the control group, one eye of each volunteer was randomly selected for statistics. In POAG patients, the eye with less severe disease was selected for statistics. SPSS 16.0 was used for statistical analysis, and $P<0.05$ was considered significant. Number of cases and percentages were used for enumeration data. Rank sum test was used for the comparison of difference in measurement data, and Chi-square test was used for the comparison of difference in enumeration data. Receiver operating characteristic (ROC) curves and area under the receiver operating characteristic (AROC) curve were used to evaluate the capability of each parameter and diagnostic model of FD-OCT in distinguishing early-stage POAG eyes from normal eyes. The method for comparing confidential interval was used to compare AROC. Total 90 healthy people and 60 early-POAG patients were randomly selected to form a modeling sample, then a combination of parameters was made with logistic regression to establish diagnostic models for early POAG. The established diagnostic models were validated by test sample that formed with the remaining healthy people and early-POAG patients.

RESULTS

Demographics of Participants The demographics of participants were shown in Table 1. For diopter, there was no significant difference between glaucoma patients and normal subjects in modeling sample (P=0.795) and test sample

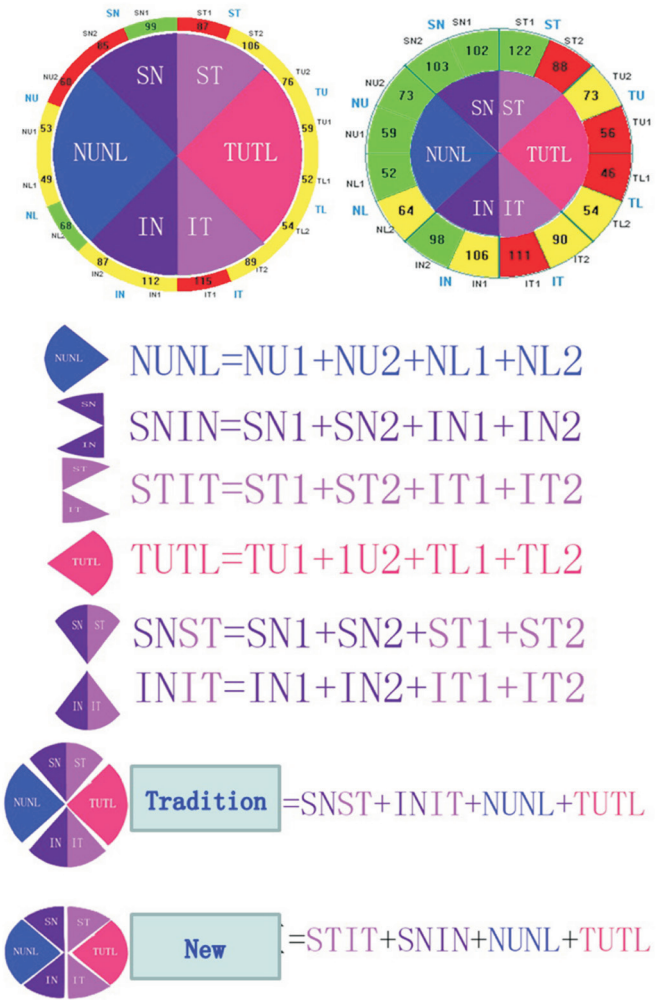

Figure 1 Area partition for RNFL thickness parameters of RNFL3.45 and ONH scan.

(P=0.640). For visual field MD and pattern standard deviation, significant differences were found between glaucoma patients and normal subjects with P=0.000 for both modeling group and test group.

Analysis of Partitioned Parameters in the Nerve Fibrous Layer Quantification of scanning parameters was necessary for the establishment of the diagnostic models. We used a scoring method for quantification of each parameter, with higher probability of abnormity in higher scores. It was scored 0 for green parameter (representing normality), and 1 for yellow parameter (representing critical status). The red parameter represented abnormality and its score should be higher than yellow, but the weight ratio between red and yellow should be calculated. Because of the difference in diagnostic values among the 6 regions, the weight ratio of the scores might differ between the yellow squares and the red ones in each region. Given 4 sectors (*i.e.* four small squares) in one region, there were five possibilities of the weight ratio between the red squares and the yellow ones, *i.e.* the weight ratio of one red square was equivalent to 1, 2, 3, 4 or more than 4 yellow squares. Therefore, when partitioned scoring was performed, it was scored 1 for the yellow squares, and 1, 2, 3,

Table 1 General information of healthy people and patients with early-stage POAG

Clinical characteristic	Modeling sample			Test sample		
	Normal subject (*n*=90)	Early-stage POAG (*n*=60)	*P*	Normal subject (*n*=43)	Early-stage POAG (*n*=39)	*P*
Diopter (D)	-1.63±1.86	-1.88±1.95	0.795	-1.31±2.23	-1.50±2.36	0.640
MD (dB)	-1.02±1.05	-3.25±1.46	0.000	-1.13±1.30	-3.24±1.64	0.000
PSD (dB)	1.53±0.51	4.20±2.40	0.000	1.59±0.42	3.63±1.95	0.000
Sex			0.000			0.067
Male	22 (39.3%)	34 (60.7%)		24 (44.4%)	30 (55.6%)	
Female	68 (72.3%)	26 (27.7%)		19 (65.5%)	10 (34.5%)	

POAG: Primary open angle glaucoma; MD: Mean deviation; PSD: Pattern standard deviation.

4 or 5 for the red ones respectively, and the score of 5 in the red square meant the weight ratio of the red square was larger than 4 yellow squares.

Each of the two types of scans including ONH and RNF3.45 comprised of 6 regions, and each region might have 5 different weight ratios when it was scored for the red squares and the yellow ones, *i.e.* the five different scoring methods. In order to define the most appropriate scoring method for each region, AROC was made for five scoring methods in each region. The results revealed that the scoring methods with the highest AROC in the 6 regions scanned with RNFL3.45 were RNUNL12, RSNIN12, RSTIT12, RTUTL12, RSTSN12, and RITIN12 respectively, and that in the 6 regions scanned with ONH were ONUNL12, OSNIN13, OSTIT12, OTUTL15, OSTSN13 and OITIN13. Table 2 showed the AROC of the best scoring method in each region, and Table 3 presented the nomenclature.

The scoring method with the highest AROC in each region was used. The 4 regions based on the traditional partition (including STSN, ITIN, NUNL and TUTL) and the new partition (including STIT, SNIN, TUTL and NUNL) were combined respectively using logistic regression model to establish two area partition diagnostic models for early-stage POAG. The models of RNFL3.45 and ONH for the traditional partition were RNFL3.45-T=RTUTL12×0.37+RSTSN12×0.65+RITIN12×0.95 and ONH-T=ONUNL12×-0.66+OSTSN13×1.51+OITIN13×1.3, and those for the new partition were RNFL3.45-N=RSTIT12 and ONH-N=OSTIT12. Table 4 presented AROC and its sensitivity, specificity, positive predictive value, negative predictive value, positive likelihood ratio and negative likelihood ratio for the 4 area partition diagnostic models.

Model Validation The 4 established models were respectively validated using the test sample. The general information of the test sample was given in Table 1. Table 5 showed the results of AROC and its sensitivity, specificity, positive predictive value, negative predictive value, positive likelihood ratio and negative likelihood ratio of the 4 models.

Table 2 The AROC of the best scoring method in each region

Scanning parameter	AROC	*P*	95% confidential interval
RSTIT12	0.966±0.017	0.000	0.933-0.998
RITIN12	0.880±0.033	0.000	0.815-0.945
RSTSN12	0.876±0.031	0.000	0.814-0.937
RSNIN12	0.873±0.031	0.000	0.813-0.933
RTUTL12	0.763±0.042	0.000	0.682-0.845
RNUNL12	0.720±0.044	0.000	0.633-0.807
OSTIT12	0.990±0.007	0.000	0.977-1.003
OSTSN13	0.896±0.031	0.000	0.836-0.955
OITIN13	0.883±0.033	0.000	0.819-0.947
OSNIN13	0.848±0.037	0.000	0.776-0.920
OTUTL15	0.787±0.041	0.000	0.706-0.868
ONUNL12	0.703±0.046	0.000	0.613-0.794

Table 3 The nomenclature of the best scoring methods in regions in RNFL3.45 and ONH

Scanning methods	Name of partition				Weight ratio between yellow and red	
RNFL3.45						
R	N	U	N	L	1	2
R	S	N	I	N	1	2
R	S	T	I	T	1	2
R	T	U	T	L	1	2
R	S	T	S	N	1	2
R	I	T	I	N	1	2
ONH						
O	N	U	N	L	1	2
O	S	N	I	N	1	2
O	S	T	I	T	1	2
O	T	U	T	L	1	2
O	S	T	S	N	1	2
O	I	T	I	N	1	2

RNFL: Retinal nerve fibre layer.

DISCUSSION

Glaucoma is characterized by a combination of structural and functional damage[13]. The structural changes in glaucoma patients usually precede functional changes[16-17]. Therefore, the most important challenge in glaucoma research is to find

Table 4 The AROC, sensitivity, specificity, PV+, PV-, LR+ and LR- for the 4 area partition diagnostic models established using the modeling samples

Models	AROC	*P*	95% confidential interval	Critical value	Sensitivity (%)	Specificity (%)	LR+	LR-	PV+ (%)	PV- (%)
RNFL3.45-T	0.956±0.018	0.000	0.921-0.990	2.33	90.0	90.0	9	0.11	95.7	93.1
ONH-T	0.990±0.006	0.000	0.978-1.000	3.14	98.3	94.4	17.55	0.02	92.2	98.8
RNFL3.45-N	0.966±0.017	0.000	0.933 -0.998	2	94.9	93.3	14.16	0.05	90.5	96.6
ONH-N	0.990±0.007	0.000	0.977-1.003	2	98.3	96.7	29.79	0.02	95.2	98.9

PV+: Positive predictive value; PV-: Negative predictive value; LR+: Positive likelihood ratio; LR-: Negative likelihood ratio.

Table 5 The AROC and its sensitivity, specificity, PV+, PV-, LR+ and LR- of the 4 models established using the test samples

Models	AROC	*P*	95% confidential interval	Critical value	Sensitivity (%)	Specificity (%)	LR+	LR-	PV+ (%)	PV- (%)
RNFL3.45-T	0.881±0.039	0.000	0.805-0.958	2.33	84.6	79.1	4.048	0.195	78.6	85.0
ONH-T	0.979±0.013	0.000	0.954-1.000	3.14	94.9	86.0	6.77	0.059	86.0	94.9
RNFL3.45-N	0.939±0.028	0.000	0.884-0.993	2	89.7	90.7	9.65	0.114	89.7	90.7
ONH-N	0.990±0.007	0.000	0.977-1.000	2	94.9	95.3	20.19	0.054	94.9	95.3

PV+: Positive predictive value; PV-: Negative predictive value; LR+: Positive likelihood ratio; LR-: Negative likelihood ratio.

the early glaucomatous structural damage. Recent developed FD-OCT technology not only has high resolution and good repeatability, but also provides both an ethnic-specific normal database with parameters (age and optic disc size) corrected and a corresponding diagnostic probability graph[18-19]. At present, we preliminarily discussed the application value of database and probability graph of Optovue RTVue100 FD-OCT in early diagnosis of POAG. Compared with our previous diagnostic model that was established based on multi-parameters, the present study focused on the different AROC between two diagnostic models based on two different area partition strategies on ONH and RNFL3.45 parameters, obtaining a more simple and practical model.

Compared with Single Parameter The AROC had been used to evaluate the diagnostic accuracy and compare the diagnostic performance of single and combined anatomic variables in many studies. Some studies suggested that combined parameters could optimize the glaucoma diagnosis[20-21]. Lu *et al*[22] performed a study to identify the best combination of Stratus OCT RNFL thickness parameters for the detection of glaucoma and found that overall average RNFL thickness had the highest AROC value of all single parameters evaluated, while the 3-parameter combination was significantly better than the overall average alone. Recent research of Wang *et al*[23] combined time-domain OCT measurements of the optic disc, circumpapillary RNFL, and macular retinal thickness to improve the diagnosis of glaucoma. They found that all combination diagnostic variables had significantly larger AROCs than any single diagnostic variable. Furthermore, some recent studies with FD-OCT also reported similar results. For instance, Fang *et al*[24] evaluated the diagnostic capability of parameters of the optic disc, RNFL thickness, and GCC using FD-OCT for early POAG patients and suggested that the combined parameters had the highest AROC.

In accordance with previous studies, our result showed that the AROC of combined diagnostic model ONH-N was 0.990, which was significantly higher than the RNFL average (AROC=0.912), the best single parameter of GCC, optic disk and RNFL scanning parameters (shown in our previous study)[15]. There sultimplied that diagnostic capability of our area partition model may be better than single parameter. Application of this model in clinical practice may be able to improve the sensitivity and specificity of FD-OCT in early diagnosis of POAG.

Comparison Between Diagnostic Models It has been reported that RNFL defect mostly occurs in inferior temporal or superior temporal in early POAG[20,25-26]. Based on the traditional partition, we introduced the novel partition, *i.e.* the combined region of STIT and SNIN. Thus points along the circumference scanned by ONH and RNFL3.45 were divided into six regions (with 4 points for each) including STIT. Among the six regions, STIT had the highest AROC.

Although there was no statistical difference between AROC among the four diagnostic models, the new partition diagnostic models (*i.e.* RNFL3.45-N, ONH-N) seemed to be simpler and more convenient in clinic. STIT12 was the only left over in the model after regression analysis. STIT12 is a parameter obtained by assigning red squares score 2 and yellow squares score 1 and summing up the scores of four squares in STIT. The sensitivity and specificity of the STIT12 score in diagnosis of early POAG was 98.3% and 96.7% respectively with the cut-off level of 2.

In our previous work, an aggregative model was established combining the parameters of RNFL, optic disc and GCC[24]. The aggregative model was more complex than the new area partition models. Overlapping of the confidential interval between them had no statistical difference. So we hold that the new area partition models are more suitable for clinical application.

Being different from previous studies[20,22-23,25,27-29], which used parameters directly coming from FD-OCT, we divided the 16 FD-OCT parameters into 6 sections and built the scoring system for each section, and then built the logistical diagnostic model using these section parameters and calculated its AROC. Thus, we could get much simpler model which was easy to use in clinic.

Verification with the Test Sample When we applied the four models in the test sample, the result showed that except for RNFL3.45-T, the AROCs of the three diagnostic models (ONH-T, RNFL3.45-N, ONH-N) were more than 0.90, suggesting a high diagnostic ability of the scoring system and diagnostic models. This result implied that the diagnostic efficiency of the diagnostic models that was recommended in the modeling sample was validated in the test sample. Overlapping of the confidential interval among the three models had no significant difference. Among them, ONH-N=OSTIT12 seemed to have the highest AROC and might be the most simplified and convenient model. Based on the result, we expected that in clinic, when a case showed 1 red square or 2 yellow squares among the four squares in STIT in the normal probability graph of RNFL parameter under the ONH scanning, doctors could make a primary diagnosis for glaucoma patient with a relative high sensitivity and specificity. It might facilitate the reading of FD-OCT scanning results to some extent and improve the application value of OCT scanning parameters in the early diagnosis of POAG, especially for non-glaucoma specialist.

In spite of no significant difference, our result showed that the AROCs of the new regional diagnostic models (ONH-N and RNFL3.45-N) were higher than that of the traditional regional diagnostic models (ONH-T and RNFL3.45-T) respectively. Besides, the AROCs of some parameters in ONH scanning (*i.e.* ONH-N) were significantly higher than that in RNFL scanning (*i.e.* RNFL3.45-T). The results may suggest not only the superiority of ONH scanning to RNFL3.45 scanning, but also the superiority of new partition models to traditional partition models in diagnostic efficiency. More researches are needed to verify the results.

In this study, we attempted to establish a scoring system and diagnostic models, using FD-OCT ethnic-specific database of normal humans, and tried to simplify and facilitate their clinical application. There are still some limitations for our research. The integral multiple was used for indexes when establishing the models, which might reduce the diagnostic efficiency of the models. In addition, the sample size in each group was a little small, especially in preperimetric glaucoma group. An expanded sample will be expected in our future study, especially for patients with preperimetric glaucoma in glaucoma group and physiologic large cup in normal group, to optimize our model for the early diagnosis of early POAG.

ACKNOWLEDGEMENTS

Authors' contributions: Conception and design of the research: Zheng YJ; Acquisition of data: Fang Y and Qiao RH; Analysis and interpretation of data: Li M and Cai Y; Statistical analysis: Li XY; Drafting the manuscript: Zheng YJ; Revision of manuscript for important intellectual content: Pan YZ.

Conflicts of Interest: Zheng YJ, None; **Pan YZ,** None; **Li XY,** None; **Fang Y,** None; **Li M,** None; **Qiao RH,** None; **Cai Y,** None.

REFERENCES

1 Rizzo MI, Greco A, De Virgilio A, Gallo A, Taverniti L, Fusconi M, Conte M, Pagliuca G, Turchetta R, de Vincentiis M. Glaucoma: recent advances in the involvement of autoimmunity. *Immunol Res* 2017;65(1):207-217.

2 Kapetanakis VV, Chan MP, Foster PJ, Cook DG, Owen CG, Rudnicka AR. Global variations and time trends in the prevalence of primary open angle glaucoma (POAG): a systematic review and meta-analysis. *Br J Ophthalmol* 2016;100(1):86-93.

3 Iwase A, Suzuki Y, Araie M; Tajimi Study Group. Characteristics of undiagnosed primary open-angle glaucoma: the Tajimi Study. *Ophthalmic Epidemiol* 2014;21(1):39-44.

4 Chen Y, Lin Y, Vithana EN, Jia L, Zuo X, Wong TY, Chen LJ, Zhu X, Tam PO, Gong B, Qian S, Li Z, Liu X, Mani B, Luo Q, Guzman C, Leung CK, Li X, Cao W, Yang Q, Tham CC, Cheng Y, Zhang X, Wang N, Aung T, Khor CC, Pang CP, Sun X, Yang Z. Common variants near ABCA1 and in PMM2 are associated with primary open-angle glaucoma. *Nat Genet* 2014;46(10):1115-1119.

5 Sommer A, Katz J, Quigley HA, Miller NR, Robin AL, Richter RC, Witt KA. Clinically detectable nerve fiber atrophy precedes the onset of glaucomatous field loss. *Arch Ophthalmol* 1991;109(1):77-83.

6 Schuman JS, Pedut-Kloizman T, Hertzmark E, *et al*. Reproducibility of nerve fiber layer thickness measurement using optical coherence tomography. *Ophthalmology* 1996;103:1889-1898.

7 Bowd C, Zangwill LM, Berry CC, Blumenthal EZ, Vasile C, Sanchez-Galeana C, Bosworth CF, Sample PA, Weinreb RN. Detecting early glaucoma by assessment of retinal nerve fiber layer thickness and visual function. *Invest Ophthalmol Vis Sci* 2001;42(9):1993-2003.

8 Pai SG, Nayak MK, Karat S. Retinal nerve fiber layer thickness in glaucomatous and normal patients using spectral domain optical coherence tomography and standard automated perimetry-a comparative analysis. *International Journal of Multidisciplinary Research and Development* 2015;2:247-251.

9 Vizzeri G, Weinreb RN, Gonzalez-Garcia AO, Bowd C, Medeiros FA, Sample PA, Zangwill LM. Agreement between spectral-domain and time-

domain OCT for measuring RNFL thickness. *Br J Ophthalmol* 2009; 93(6):775-781.

10 Schuman JS. Spectral domain optical coherence tomography for glaucoma (an AOS thesis). *Trans Am Ophthalmol Soc* 2008;106:426-458.

11 Leung CKS, Shi L, Weinreb RN, *et al*. Retinal nerve fiber layer imaging with spectral-domain optical coherence tomography: analysis of the retinal nerve fiber layer map for glaucoma detection. *Ophthalmology* 2010;117:1684-1691.

12 Leung CK, Chiu V, Weinreb RN, Liu S, Ye C, Yu M, Cheung CY, Lai G, Lam DS. Evaluation of retinal nerve fiber layer progression in glaucoma: a comparison between spectral-domain and time-domain optical coherence tomography. *Ophthalmology* 2011;118(8):1558-1562.

13 Wollstein G, Schuman JS, Price LL, Aydin A, Stark PC, Hertzmark E, Lai E, Ishikawa H, Mattox C, Fujimoto JG, Paunescu LA. Optical coherence tomography longitudinal evaluation of retinal nerve fiber layer thickness in glaucoma. *Arch Ophthalmol* 2005;123(4):464-470.

14 Sidharta S, Puri R, Frost L, Kataoka Y, Carbone A, Willoughby S, Nelson A, Nicholls S, Worthley S, Worthley M. The impact of lumen size and microvascular resistance on Fourier-domain optical coherence tomography (FD-OCT) coronary measurements. *Int J Cardiol* 2014;174(1):210-211.

15 Zheng Y, Pan Y. Application of the frequency-domain optical coherence tomography database of normal humans in the diagnosis of primary open-angle glaucoma. *Chinese Journal of Optometry Ophthalmology and Visual science* 2015;17:538-544.

16 Sommer A, Pollack I, Maumenee AE. Optic disc parameters and onset of glaucomatous field loss. I. Methods and progressive changes in disc morphology. *Arch Ophthalmol* 1979;97(8):1444-1448.

17 Kass MA, Heuer DK, Higginbotham EJ, Johnson CA, Keltner JL, Miller JP, Parrish RK 2nd, Wilson MR, Gordon MO. The Ocular Hypertension Treatment Study: a randomized trial determines that topical ocular hypotensive medication delays or prevents the onset of primary open-angle glaucoma. *Arch Ophthalmol* 2002;120(6):701-713;discussion 829-830.

18 Chen TC, Cense B, Pierce MC, Nassif N, Park BH, Yun SH, White BR, Bouma BE, Tearney GJ, de Boer JF. Spectral domain optical coherence tomography: ultra-high speed, ultra-high resolution ophthalmic imaging. *Arch Ophthalmol* 2005;123(12):1715-1720.

19 Kim JS, Ishikawa H, Sung KR, Xu J, Wollstein G, Bilonick RA, Gabriele ML, Kagemann L, Duker JS, Fujimoto JG, Schuman JS. Retinal nerve fibre layer thickness measurement reproducibility improved with spectral domain optical coherence tomography. *Br J Ophthalmol* 2009;93(8):1057-1063.

20 Chen HY, Huang ML, Hung PT. Logistic regression analysis for glaucoma diagnosis using stratus optical coherence tomography. *Optom Vis Sci* 2006;83(7):527-534.

21 Burgansky-Eliash Z, Wollstein G, Chu T, Ramsey JD, Glymour C, Noecker RJ, Ishikawa H, Schuman JS. Optical coherence tomography machine learning classifiers for glaucoma detection: a preliminary study. *Invest Ophthalmol Vis Sci* 2005;46:4147-4152.

22 Lu AT, Wang M, Varma R, Schuman JS, Greenfield DS, Smith SD, Huang D; Advanced Imaging for Glaucoma Study Group. Combining nerve fiber layer parameters to optimize glaucoma diagnosis with optical coherence tomography. *Ophthalmology* 2008; 115(8):1352-1357.

23 Wang M, Lu AT, Varma R, Schuman JS, Greenfield DS, Huang D. Combining information from 3 anatomic regions in the diagnosis of glaucoma with time-domain optical coherence tomography. *J Glaucoma* 2014;23(3):129-135.

24 Fang Y, Pan YZ, Li M, Qiao RH, Cai Y. Diagnostic capability of Fourier-Domain optical coherence tomography in early primary open angle glaucoma. *Chin Med J* 2010;123(15):2045-2050.

25 Budenz DL, Michael A, Chang RT, McSoley J, Katz J. Sensitivity and specificity of the StratusOCT for perimetric glaucoma. *Ophthalmology* 2005;112(1):3-9.

26 Sihota R, Sony P, Gupta V, Dada T, Singh R. Comparing glaucomatous optic neuropathy in primary open angle and chronic primary angle closure glaucoma eyes by optical coherence tomography. *Ophthalmic Physiol Opt* 2005;25(5):408-415.

27 Mwanza JC, Warren JL, Budenz DL; Ganglion Cell Analysis Study Group. Combining spectral domain optical coherence tomography structural parameters for the diagnosis of glaucoma with early visual field loss. *Invest Ophthalmol Vis Sci* 2013;54(13):8393-8400.

28 Medeiros FA, Zangwill LM, Bowd C, Vessani RM, Susanna R Jr, Weinreb RN. Evaluation of retinal nerve fiber layer, optic nerve head, and macular thickness measurements for glaucoma detection using optical coherence tomography. *Am J Ophthalmol* 2005;139(1):44-55.

29 Huang JY, Pekmezci M, Mesiwala N, Kao A, Lin S. Diagnostic power of optic disc morphology, peripapillary retinal nerve fiber layer thickness, and macular inner retinal layer thickness in glaucoma diagnosis with fourier-domain optical coherence tomography. *J Glaucoma* 2011;20(2):87-94.